Original Research

Physiological Noise in MR Images: An Indicator of the Tissue Response to Ischemia?

Harris H. Wang, SB,[1] Nina M. Menezes, PhD,[2] Ming Wang Zhu, MD,[2] Hakan Ay, MD,[2,3] Walter J. Koroshetz, MD,[3] Hannu J. Aronen, MD, PhD,[4–6] Jari O. Karonen, MD, PhD,[7,8] Yawu Liu, MD, PhD,[7,8] Juho Nuutinen, MD,[7,8] Lawrence L. Wald, PhD,[2] and A. Gregory Sorensen, MD[1,2*]

Purpose: To determine whether measuring signal intensity (SI) fluctuations in MRI time series data from acute stroke patients would identify ischemic tissue.

Materials and Methods: Prebolus perfusion-weighted MRI data from 32 acute ischemic stroke patients ($N = 32$) was analyzed as a time series. Ischemic and normal tissue regions were outlined and compared.

Results: The magnitude of the measured SI fluctuations was significantly lower in ischemic regions relative to normal tissue. Spatial differences in these fluctuations occurred in a manner that was different than other perfusion-based metrics.

Conclusion: Prior studies have shown that SI fluctuations in MRI time series data correspond to the presence of physiological "noise," which includes vasomotion, an autoregulatory phenomenon that affects the tissue response to ischemia. In this study, SI fluctuations were found to decrease in ischemia, consistent with the notion that small vessels will remain open (fluctuations in vessel diameter will decrease) when there is a challenge to flow. Spatial variation in SI fluctuations appeared to be different from spatial variation seen on other perfusion-based metrics, suggesting that a separate contrast mechanism is responsible, one that might be of diagnostic and prognostic value in acute stroke in which the ability of tissue to withstand ischemia is currently not well visualized.

Key Words: stroke; ischemia; MRI; vasomotion; noise
J. Magn. Reson. Imaging 2008;27:866–871.

SPONTANEOUS low frequency oscillations (<0.1 Hz) in regional cerebral blood flow (CBF) and oxygenation have been observed using blood oxygen level dependent (BOLD) MRI time series measurements in the so-called "resting state," i.e., in the absence of any functional task (Fig. 1) (1–6). The frequency of these fluctuations is much lower than those attributed to cardiac motion and respiration (with fundamental frequencies at approximately 1 Hz and 0.2–0.3 Hz, respectively). Together, these three frequency components constitute the small physiological signals, sometimes referred to as physiological "noise," in MRI time series data, modulating signal intensity (SI). Numerous techniques have been developed to isolate and remove this and other physiological noise components from BOLD data (7–10) and, although the biological basis of the low frequency component of physiological noise is not completely understood, it is believed to correspond to arteriolar vasomotion, an adaptive hemodynamic response that helps regulate blood flow. Indeed, the low-frequency component found in MRI time series data corresponds to the frequency attributed to arteriolar vasomotion and has been found to be synchronized between linked brain regions, suggesting neuronal mediation, and hence a link to neuronal viability.

Vasomotion is the rhythmic oscillation in vascular diameter or tone caused by local changes in vascular smooth muscle contraction and dilation, and differs from oscillations caused by pulse, respiration, and neuronal activity. Vasomotion is thought to occur normally

[1]Medical Engineering Medical Physics Program, Division of Health Sciences and Technology, Harvard University–Massachusetts Institute of Technology, Cambridge, Massachusetts, USA.
[2]Athinoula A. Martinos Center for Biomedical Imaging, Department of Radiology, Massachusetts General Hospital, Boston, Massachusetts, USA.
[3]Stroke Service, Department of Neurology, Massachusetts General Hospital, Boston, Massachusetts, USA.
[4]Functional Brain Imaging Unit, Helsinki Brain Research Center, Helsinki, Finland.
[5]Centre for Military Medicine, Finnish Defence Forces, Helsinki, Finland.
[6]Department of Diagnostic Radiology, University of Turku, Turku, Finland.
[7]Department of Clinical Radiology, Kuopio University Hospital, Kuopio, Finland.
[8]Department of Neurology, Kuopio University Hospital, Kuopio, Finland.
Contract grant sponsor: Mental Illness and Neuroscience Discovery Institute; Contract grant sponsor: Public Health Service; Contract grant number: NS38477; Contract grant sponsor: National Center for Research Resources; Contract grant number: P41RR14075.
*Address reprint requests to: A.G.S., Massachusetts General Hospital, Building 149, 13th Street (2301), Boston, MA 02129.
E-mail: sorensen@nmr.mgh.harvard.edu
Received March 21, 2006; Accepted February 22, 2007.
DOI 10.1002/jmri.21007
Published online in Wiley InterScience (www.interscience.wiley.com).

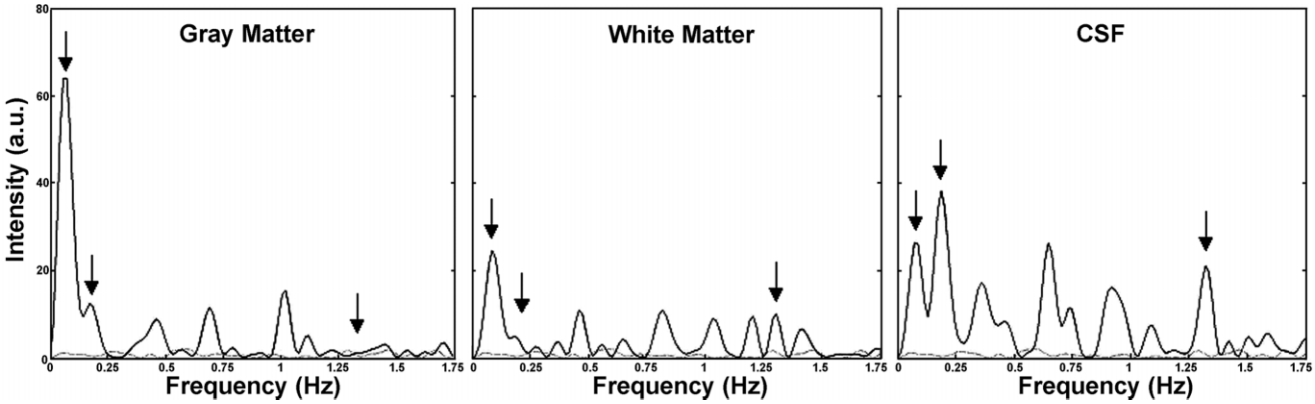

Figure 1. Power spectra corresponding to a gray matter voxel, a white matter voxel, and a CSF voxel produced by performing time-domain fast Fourier transforms on time series data collected on a normal volunteer using a short TR acquisition (TR/TE = 136 msec/54 msec, single axial slice = 256 images). Note the different peaks corresponding to presumed sources of physiological noise (arrows) and their harmonics: vasomotion (approximately 0.1 Hz), respiration (0.2 Hz), and cardiac motion (1.3 Hz). The frequencies of respiration and cardiac noise spectral components were determined by measuring the subject's respiratory and heart rates; the frequency of vasomotion is estimated based on published values. Low-frequency fluctuations (presumed to correspond to vasomotion) appear to be more prominent in gray matter and CSF than in white matter. Respiration and cardiac motion appear to be most pronounced in CSF. The faint dotted line in each plot corresponds to the spectrum of a background voxel. Data such as this (i.e., long time series with a short TR) was not available in our clinical stroke cohort.

and varies in response to the tissue's demand for oxygen. Thus, one might expect that vasomotion would be altered in ischemia, with the microvasculature maximally dilated. Studies have confirmed that the amplitude of synchronized fluctuations decreases (consistent with the notion that the arterioles remain open) in response to altered brain perfusion due to hypotension, hyperventilation, cerebral artery occlusion, and cerebral vasoconstriction (3,11). Furthermore, fluctuations were found to be absent in severely ischemic brain regions (11). Thus, measurements of vasomotion appear likely to be of potential diagnostic and prognostic value in determining tissue fate in acute stroke.

Currently, imaging in the acute phase of ischemic stroke is used to establish or confirm the diagnosis and to exclude hemorrhage. Much research has focused on utilizing imaging to differentiate between ischemic tissue that is potentially salvageable and tissue that is irreversibly injured. To this end, diffusion-weighted and perfusion-weighted MRI (DWI and PWI, respectively) techniques have shown great utility in acute stroke (12–24), helping to define the abnormally perfused territory and depicting the tissue that is likely to infarct. However, the natural history of abnormally perfused tissue is highly variable and this variability is not fully determined by DWI and PWI parameters. Measuring vasomotion could complement existing MRI techniques used in stroke by providing a much needed window into the ability of tissue to withstand ischemia.

In this study, we analyzed prebolus PWI MR images from stroke patients as time series data and quantified physiological noise by measuring the shot-to-shot variation in the time series SI, calculated via the standard deviation (SD). PWI is performed routinely in the acute stroke setting to visualize the extent of the ischemic territory and, therefore, is readily available for further analyses. PWI consists of a time series of T2*-weighted images, similar in this sense to BOLD data in which low frequency fluctuations have been observed. In order to avoid confounds due to the contrast bolus, we limited our examination to the prebolus segment. The goal of this pilot study was to determine whether measures of physiological noise in this data would identify ischemic tissue. Specifically, we sought to determine: 1) whether there is any spatial structure to maps that quantify SI fluctuations (a measure of physiological noise) in acute stroke prebolus PWI; 2) whether any such spatial variation corresponds to tissue at risk of infarction on follow-up; and 3) whether this spatial variation is different than the commonly calculated PWI metrics of mean transit time (MTT), CBF, and cerebral blood volume (CBV).

MATERIALS AND METHODS

This was a retrospective study of consecutively-acquired patient data sets. To be included in the study, ischemic stroke patients had to have undergone PWI within 12 hours of symptom onset, follow-up T2 imaging a minimum of five days after symptom onset, and no visually appreciable gross head motion on PWI. A total of 32 patients with anterior MCA ischemic stroke were included (17 men and 15 women), with Institutional Review Board approval. The average age of the patients was 67 years. The average time to MRI was 6.5 hours.

MR images were acquired as follows. Axial single-shot echo-planar images were acquired during the first pass of 0.2 mmol/kg of a gadolinium-based contrast agent injected 10 seconds after the start of imaging at a rate of 5 mL/second with use of an MRI-compatible power injector (Medrad, Pittsburgh, PA, USA). The contrast agent was followed by a comparable volume of normal saline injected at the same rate of 5 mL/second. Datasets consisted of 7–11 slices over 40–80 time points at 1.5 T. A fixed field of view (FOV) of 220 × 220 mm and an acquisition matrix of 128 × 128 pixels were used.

Table 1
Normal Differences

	No. of patients	Average difference in σ_{SI}^2
White < gray	31	11.4 ± 4.3%
White = gray	1	N/S
White > gray	0	
Total	32	

NS = not significant.

Slice thickness was 5–6 mm and TR/TE = 1500/65–78 msec.

Because of the low number of prebolus images in these PWI series, it was not possible to perform a Fourier transform analysis, filtering for the low frequency component. Instead, MRI SI fluctuations were quantified by calculating the SD of the prebolus perfusion images (σ_{SI}). The number of images varied from patient to patient, 17 images on average. σ_{SI}^2 was calculated on a voxel-by-voxel basis to produce maps. The first two images were excluded from the σ_{SI}^2 calculation because they often showed different SIs due to transient magnetization, leaving approximately 15 images used to generate each patient's σ_{SI}^2 map. To avoid introducing artifacts in calculating σ_{SI}^2, no filtering, data fitting, or motion correction algorithms were used (5).

Concentrations vs. time curves were extrapolated from the perfusion images on a voxel-by-voxel basis. Integrating the curve over time produces values proportional to CBV. CBF was then computed using deconvolution techniques (25). From the central volume theorem, MTT was then calculated as MTT = CBV/CBF.

A neuroradiologist blinded to the follow-up images outlined areas of abnormal MTT representing the acute lesion and the outlines were transferred to the σ_{SI}^2 maps. Lesions were additionally manually subdivided into gray and white matter with the help of the first image in the perfusion series, excluding voxels containing CSF or those from blood vessels. Healthy gray and white matter were also manually outlined. Voxels pertaining to one of the four subgroups (lesion white, lesion gray, normal white, and normal gray) in all slices were pooled for each patient, and statistical tests were done to compare differences between these pools of voxels for each patient. The difference between lesion gray and normal gray matter, as well as lesion white and normal white matter, was calculated for each patient. Student's *t*-test was then applied to the gray and white matter σ_{SI}^2 differences on a patient-by-patient basis to determine whether they were significant (P = 0.05). This process was then repeated using CBF and then CBV maps to identify the acute lesion.

Areas of abnormal T2, representing the final infarct, were also outlined for each patient and the outlines transferred to the σ_{SI}^2 maps. We compared gray and white matter in the regions that were "missed" on acute PWI (i.e., those regions that appeared normal on acute perfusion imaging but went onto infarct on follow-up T2) to normal tissue (i.e., tissue that was normal on acute DWI and PWI as well as on follow-up T2 images).

RESULTS

Normal Variation

We observed variations in the σ_{SI}^2 maps that generally corresponded to a spatial pattern. In normal sections, this spatial pattern corresponded to gray-white contrast. For 31 of 32 patients, normal white matter voxels had significantly lower average σ_{SI}^2 than voxels of normal gray matter (P = 0.05, Table 1). This difference, as high as 20% in some cases, was 11.4 ± 4.3% on average. An example of a normal brain slice, showing the difference in σ_{SI}^2 between white and gray matter, is shown in Fig. 2. For the remaining patient, the average σ_{SI}^2 in voxels of normal white matter was not statistically different than the average σ_{SI}^2 in voxels of normal gray matter.

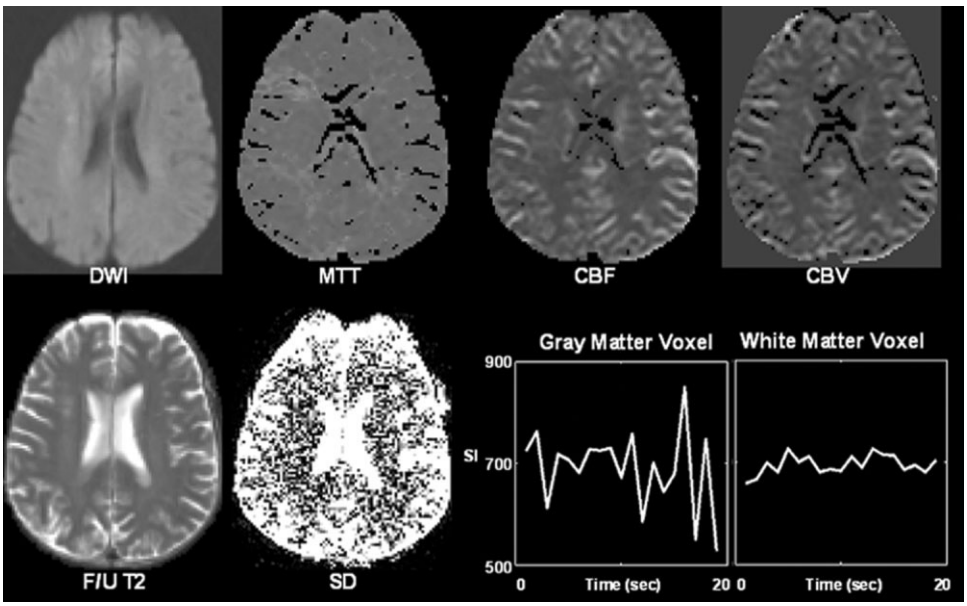

Figure 2. An example of a normal brain slice from a stroke patient who showed decreased σ_{SI}^2 in normal white matter relative to normal gray matter. The σ_{SI}^2 map was maximally windowed to best show the differences between white and gray matter. Also shown are acute DWI, MTT, CBF, CBV, and follow-up T2 images. SI vs. time curves for a normal gray matter voxel and a normal white matter voxel are plotted. These clearly show decreased fluctuations normally found in white matter relative to gray.

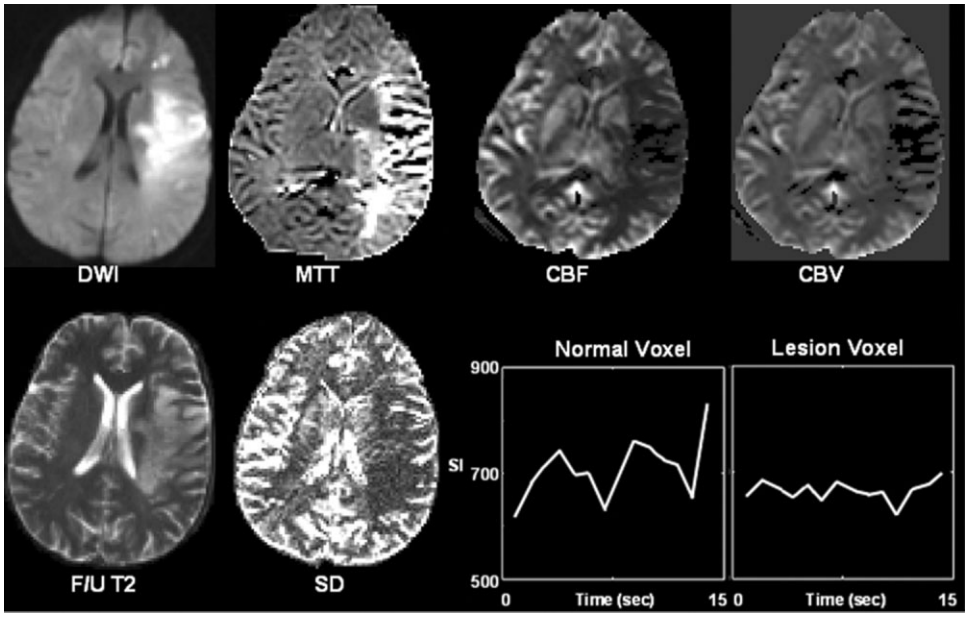

Figure 3. A typical stroke patient who showed decreased σ_{SI}^2 in the acute PWI lesion. The σ_{SI}^2 map is shown along with acute DWI, MTT, CBF, CBV, and follow-up T2 images. Also shown are SI vs. time curves for a normal gray matter voxel and an ischemic gray matter voxel. Note the decrease in fluctuations in the ischemic time series relative to normal as well as the lower intensity in the ischemic region on the σ_{SI}^2 map.

Ischemic Differences

Figure 3 is an example of a brain slice with a lesion, showing the difference in σ_{SI}^2 between normal tissue and the lesion. There were often no obvious boundaries on the σ_{SI}^2 maps between normal tissue and the lesion. We therefore used MTT, CBF, and CBV maps to select regions of interest in order to assess whether σ_{SI}^2 reflects ischemia. Table 2 summarizes the differences in σ_{SI}^2 between voxels in the lesion as identified on acute MTT maps and voxels identified as normal tissue. Because of the differences in σ_{SI}^2 seen normally between gray and white matter, we analyzed these two tissue types separately. We found that for gray matter, MTT lesion σ_{SI}^2 was lower than normal in most patients (20/32) by approximately 6.4% on average. We found that for white matter, the average σ_{SI}^2 in lesion voxels was often lower than average σ_{SI}^2 in normal voxels (11 patients), but, equally often, not significantly different than normal (11 patients).

Table 3 summarizes the findings for the average σ_{SI}^2 in lesion voxels compared to normal voxels when CBF was used to define the acute lesion. For gray matter, average lesion σ_{SI}^2 was lower than normal for most (25 of 32), but not all (7/32), cases. For white matter, average lesion σ_{SI}^2 was not clearly distinguishable from the average σ_{SI}^2 in normal voxels as often as it was lower than in normal voxels (lower average σ_{SI}^2 in 13 patients, similar in 19 patients). Table 4 summarizes the findings for σ_{SI}^2 lesion compared to normal when CBV was used to define the acute lesion. For gray matter, average σ_{SI}^2 in lesion voxels was lower than average σ_{SI}^2 in normal voxels for only half of the cases (15/30).

In addition, we examined σ_{SI}^2 maps for their ability to detect ischemia in regions that appeared normal on all acute PWI maps but went onto infarct on follow-up T2 (termed "missed" regions). For gray matter, σ_{SI}^2 was able to reflect abnormalities consistent with ischemia in missed regions in at least half of the cases (Table 5) for MTT, CBF, and CBV, demonstrating that σ_{SI}^2 contains information beyond that seen on acute PWI. These findings were not observed in white matter (data not shown).

DISCUSSION

In conclusion, we report a novel contrast mechanism to visualize brain ischemia. SD (σ_{SI}^2) maps of MRI time series data, which quantify noise, including noise from physiological sources, appear to contain spatial structure, vary with tissue type and pathology, and differ from PWI metrics calculated from, in part, the same underlying imaging data. To our knowledge, this is the first report of an investigation into the utility of measuring physiological noise in MRI data in stroke. Our work supports earlier reports of low frequency signal fluctuations consistent with physiologic vasomotion in

Table 2
Comparison Using MTT

Gray matter	No. of patients	Average difference in σ_{SI}^2
Lesion < normal	20	−6.4 ± 6.2%
Lesion = normal	6	N/S
Lesion > normal	6	4.3 ± 2.7%
Total	32	

N/S = not significant.

Table 3
Comparison Using CBF

Gray matter	No. of patients	Average difference in σ_{SI}^2
Lesion < normal	25	−5.4 ± 5.0%
Lesion = normal	6	N/S
Lesion > normal	1	3.2%
Total	32	

N/S = not significant.

the brain. In extending this type of analysis to patients with acute ischemic stroke, we report that σ_{SI}^2 appears to be a novel contrast mechanism to visualize ischemic tissue. We found that σ_{SI}^2 maps of prebolus perfusion images show spatial variation both between normal gray and white matter, and also between ischemic and normal tissue. Because thermal and scanner noise do not typically correspond to any particular spatial distribution, we speculate that the regional differences seen on the σ_{SI}^2 maps are due to physiological noise. Furthermore, because we do not expect to find differences from bulk cardiac (26) and/or respiratory motion in ischemic regions relative to normal, we propose that the spatial differences we observed in σ_{SI}^2 are due to the vasomotion component of physiological noise.

We expect that, while related, σ_{SI}^2 maps should provide different information than CBF since one may be more sensitive to the microvasculature while the other may be more sensitive to the macrovasculature. If this is not the case, then σ_{SI}^2 may provide a nonexogenous-contrast method of measuring CBF. We found that σ_{SI}^2 indicated the same threatened tissue as CBF in most (25/32), but not all, patients (7/32). In addition, σ_{SI}^2 was sensitive to tissue at risk "missed" on CBF in seven out of 12 patients in whom "missed" regions were observed. While these findings need to be confirmed in a larger cohort, this suggests that σ_{SI}^2 and CBF provide different information.

One limitation to our pilot study is its retrospective nature. In addition to the unknown biases that can arise from retrospective studies, a shortcoming is the frequency of the prebolus PWI images was not sufficiently high (i.e., the TR was 1.5 seconds) to avoid aliasing of the cardiac peak (approximately 1 Hz), and the limited number of prebolus images made it unfeasible to perform more sophisticated analyses (i.e., spectral filtering methods) to isolate the low frequency component of the signal (as performed for the subject shown in Fig. 1). With this relatively slow sampling rate and limited number, the power spectrum of the noise is not well populated. Thus, we cannot state with certainty that the σ_{SI}^2 differences we see in the brain are due to processes occurring at the 0.1 Hz rate that has been speculated to correspond to vasomotion. While vasomotion differences could easily be responsible for the σ_{SI}^2 variation we observed, a higher sampling rate (to avoid aliasing of the cardiac signal) and more images (to improve the signal-to-noise ratio [SNR]) are required to confirm this. It should also be noted that there are other physiological processes besides vasomotion that have been measured as occurring at or near 0.1 Hz. For instance, low-frequency oscillations in blood pressure occur in the vicinity of 0.1 Hz. Regardless of the precise physiological processes responsible for the spatial variation in our "noise" measurements, the fact that this variation appears to correspond to pathology confirms that such measurements have potential clinical utility and therefore warrant further investigation. Our results, therefore, point clearly to a need for further studies but also provide the motivation for such studies.

Newer techniques that purportedly investigate the status of the microvasculature, such as spin echo, dual echo interleaved spin echo, and gradient echo acquisitions, may help further isolate the vasomotion contribution to physiological noise. Recently, postprocessing techniques to develop CBF maps based on multiple localized arterial input functions were developed (27,28), which may additionally improve our ability to visualize the status of the microvasculature. Furthermore, improved acquisition techniques such as the use of eight-channel receivers and 3T (or 7T) imaging, which may result in less machine noise, will likely improve sensitivity to physiological noise (29,30).

Table 4
Comparison Using CBV

Gray matter	No. of patients	Average difference in σ_{SI}^2
Lesion < normal	15	−5.1 ± 3.3%
Lesion = normal	10	N/S
Lesion > normal	5	5.1 ± 3.0%
Total	30	

N/S = not significant.

Table 5
Comparison Using "Missed" Regions (Gray Matter Only)

	No. of patients	Average difference in σ_{SI}^2
MTT		
Missed < normal	5	−6.2 ± 2.4%
Missed = normal	1	N/S
Missed > normal	3	14.3 ± 17.9%
Total	9	
CBF		
Missed < normal	7	−5.9 ± 2.4%
Missed = normal	2	N/S
Missed > normal	3	13.2 ± 13.4%
Total	12	
CBV		
Missed < normal	7	−5.1± 1.8%
Missed = normal	0	N/S
Missed > normal	4	11.1 ± 9.7%
Total	11	

N/S = not significant.

REFERENCES

1. Hyde J, Biswal B. Functionally related correlation in the noise. In: Functional MRI (Moonen CT, Bandettini PA, Eds.), Berlin: Springer Verlag; 2000;263–275.
2. Biswal B, Yetkin FZ, Haughton VM, Hyde JS. Functional connectivity in the motor cortex of resting human brain using echo-planar MRI. Magn Reson Med 1995;34:537–541.
3. Biswal B, Hudetz AG, Yetkin FZ, Haughton VM, Hyde JS. Hypercapnia reversibly suppresses low-frequency fluctuations in the human motor cortex during rest using echo-planar MRI. J Cereb Blood Flow Metab 1997;17:301–308.
4. Biswal BB, Van Kylen J, Hyde JS. Simultaneous assessment of flow and BOLD signals in resting-state functional connectivity maps. NMR Biomed 1997;10:165–170.
5. Lowe MJ, Mock BJ, Sorenson JA. Functional connectivity in single and multislice echoplanar imaging using resting-state fluctuations. Neuroimage 1998;7:119–132.
6. Cordes D, Haughton VM, Arfanakis K, et al. Frequencies contributing to functional connectivity in the cerebral cortex in "resting-state" data. AJNR Am J Neuroradiol 2001;22:1326–1333.
7. Hu X, Le TH, Parrish T, Erhard P. Retrospective estimation and correction of physiological fluctuation in functional MRI. Magn Reson Med 1995;34:201–212.

8. Biswal B, DeYoe AE, Hyde JS. Reduction of physiological fluctuations in fMRI using digital filters. Magn Reson Med 1996;35:107–113.
9. Wowk B, McIntyre MC, Saunders JK. k-Space detection and correction of physiological artifacts in fMRI. Magn Reson Med 1997; 38:1029–1034.
10. Glover GH, Li TQ, Ress D. Image-based method for retrospective correction of physiological motion effects in fMRI: RETROICOR. Magn Reson Med 2000;44:162–167.
11. Hudetz AG, Biswal BB, Shen H, Lauer KK, Kampine JP. Spontaneous fluctuations in cerebral oxygen supply. An introduction. Adv Exp Med Biol 1998;454:551–559.
12. Sorensen AG, Buonanno FS, Gonzalez RG, et al. Hyperacute stroke: evaluation with combined multisection diffusion- weighted and hemodynamically weighted echo-planar MR imaging. Radiology 1996;199:391–401.
13. Warach S, Dashe JF, Edelman RR. Clinical outcome in ischemic stroke predicted by early diffusion- weighted and perfusion magnetic resonance imaging: a preliminary analysis. J Cereb Blood Flow Metab 1996;16:53–59.
14. Beaulieu C, de Crespigny A, Tong DC, Moseley ME, Albers GW, Marks MP. Longitudinal magnetic resonance imaging study of perfusion and diffusion in stroke: evolution of lesion volume and correlation with clinical outcome. Ann Neurol 1999;46:568–578.
15. Darby DG, Barber PA, Gerraty RP, et al. Pathophysiological topography of acute ischemia by combined diffusion- weighted and perfusion MRI. Stroke 1999;30:2043–2052.
16. Neumann-Haefelin T, Wittsack HJ, Wenserski F, et al. Diffusion- and perfusion-weighted MRI. The DWI/PWI mismatch region in acute stroke. Stroke 1999;30:1591–1597.
17. Schlaug G, Benfield A, Baird AE, et al. The ischemic penumbra: operationally defined by diffusion and perfusion MRI. Neurology 1999;53:1528–1537.
18. Kluytmans M, van Everdingen KJ, Kappelle LJ, Ramos LM, Viergever MA, van der Grond J. Prognostic value of perfusion- and diffusion-weighted MR imaging in first 3 days of stroke. Eur Radiol 2000;10:1434–1441.
19. Schellinger PD, Fiebach JB, Jansen O, et al. Stroke magnetic resonance imaging within 6 hours after onset of hyperacute cerebral ischemia. Ann Neurol 2001;49:460–469.
20. Rohl L, Ostergaard L, Simonsen CZ, et al. Viability thresholds of ischemic penumbra of hyperacute stroke defined by perfusion-weighted MRI and apparent diffusion coefficient. Stroke 2001;32: 1140–1146.
21. Rose SE, Chalk JB, Griffin MP, et al. MRI based diffusion and perfusion predictive model to estimate stroke evolution. Magn Reson Imaging 2001;19:1043–1053.
22. Wu O, Koroshetz WJ, Ostergaard L, et al. Predicting tissue outcome in acute human cerebral ischemia using combined diffusion- and perfusion-weighted MR imaging. Stroke 2001;32:933–942.
23. Schaefer PW, Hunter GJ, He J, et al. Predicting cerebral ischemic infarct volume with diffusion and perfusion MR imaging. AJNR Am J Neuroradiol 2002;23:1785–1794.
24. Wittsack HJ, Ritzl A, Fink GR, et al. MR imaging in acute stroke: diffusion-weighted and perfusion imaging parameters for predicting infarct size. Radiology 2002;222:397–403.
25. Ostergaard L, Sorensen AG, Kwong KK, Weisskoff RM, Gyldensted C, Rosen BR. High resolution measurement of cerebral blood flow using intravascular tracer bolus passages. Part II: Experimental comparison and preliminary results. Magn Reson Med 1996;36: 726–736.
26. Dagli MS, Ingeholm JE, Haxby JV. Localization of cardiac-induced signal change in fMRI. Neuroimage. 1999;9:407–415.
27. Calamante F, Morup M, Hansen LK. Defining a local arterial input function for perfusion MRI using independent component analysis. Magn Reson Med 2004;52:789–797.
28. Lorenz C, Benner T, Chen PJ, et al. Automated perfusion-weighted MRI using localized arterial input functions. J Magn Reson Imaging 2006;24:1133–1139.
29. Triantafyllou C, Hoge RD, Krueger G, et al. Comparison of physiological noise at 1.5 T, 3 T and 7 T and optimization of fMRI acquisition parameters. Neuroimage 2005;26:243–250.
30. Kruger G, Glover GH. Physiological noise in oxygenation-sensitive magnetic resonance imaging. Magn Reson Med 2001;46:631–637.